

See discussions, stats, and author profiles for this publication at: <https://www.researchgate.net/publication/49691217>

Line Emission of Sodium and Hydroxyl Radicals in Single-Bubble Sonoluminescence

ARTICLE in THE JOURNAL OF PHYSICAL CHEMISTRY A · JANUARY 2011

Impact Factor: 2.69 · DOI: 10.1021/jp1083339 · Source: PubMed

CITATIONS

7

READS

29

5 AUTHORS, INCLUDING:



Julia Schneider

Georg-August-Universität Göttingen

8 PUBLICATIONS 20 CITATIONS

SEE PROFILE



Rachel Pflieger

Institut de Chimie Séparative de Marcoule

32 PUBLICATIONS 188 CITATIONS

SEE PROFILE



Sergey Nikitenko

Atomic Energy and Alternative Energies Co...

79 PUBLICATIONS 1,220 CITATIONS

SEE PROFILE



Helmuth Moehwald

Max Planck Institute of Colloids and Interfa...

1,002 PUBLICATIONS 38,571 CITATIONS

SEE PROFILE

Line Emission of Sodium and Hydroxyl Radicals in Single-Bubble Sonoluminescence

Julia Schneider,[†] Rachel Pflieger,^{*,‡} Sergey I. Nikitenko,[‡] Dmitry Shchukin,[†] and Helmuth Möhwald[†]

Max Planck Institute of Colloids and Interfaces, Am Mühlenberg 1, 14476 Potsdam, Germany and Marcoule Institute for Separation Chemistry (ICSM), UMR 5257, BP 17171-30207 Bagnols-sur-Cèze Cedex France

Received: September 1, 2010; Revised Manuscript Received: November 23, 2010

Spectroscopic studies of single-bubble sonoluminescence (SBSL) in water and aqueous sodium chloride solutions with a defined concentration of argon were performed as a function of the driving acoustic pressure. The broad-band continuum ranging from 200 to 700 nm is characterized by fits using Planck's law of blackbody radiation. The obtained blackbody temperatures are in the range of 10^4 K and are revealed to be independent of the presence of a salt and the acoustic pressure, whereas the SL intensity increases by a factor of more than 10 within the studied acoustic pressure range. The different trends followed by SL intensity and blackbody temperatures question the blackbody model. In solutions with 70 mbar of argon, line emissions of OH[•] radicals and Na^{*} are observed. The shape of the OH[•] radical emission spectrum is very similar to that in MBSL spectra, indicating the strong similarity of intrabubble conditions. An increase of the acoustic pressure causes the continuum to overlap the lines until they become indistinguishable. The emission line of Na^{*} in NaCl is observed only at high NaCl concentrations. When sodium dodecylsulfate is used a pronounced Na^{*} line is already observed in a 1 mM solution thanks to enrichment of sodium ions at the interface. The results presented in this work reveal the strong similarity of SBSL and MBSL under certain experimental conditions.

Introduction

Ultrasound-induced cavitation has several well-studied physical and chemical effects such as acoustic streaming, turbulence, acoustic wave attenuation, reflection and scattering, jet formation, cavitation bioeffects, surface erosion, and sonochemical effects involving generation of reactive chemical species.¹ Another very thoroughly studied effect going along with cavitation is the emission of a characteristic UV–visible light pulse named sonoluminescence (SL). SL can be generated either from a cloud of cavitation bubbles, known as multibubble sonoluminescence (MBSL),² or from a single bubble, termed single-bubble sonoluminescence (SBSL).^{3,4} In both cases the light pulse indicates the generation of hot spot(s) with high temperatures and pressures, suggesting the presence of active molecular and atomic species in its core, at its interface, and/or in the adjacent liquid layer. It is generally accepted that the origin of the light emission is a combination of plasma and emission from excited species.^{5–7}

Mechanisms leading to MBSL and SBSL were long considered as different since MBSL spectra are composed of a broad continuum that can exhibit characteristic atomic and molecular emission lines in the presence of noble gases and spectroscopic active solutes, whereas SBSL spectra were long considered as consisting of a sole continuum.⁸ New perspectives to study SBSL were opened by the recent works of Young⁹ and Liang,¹⁰ who determined the experimental conditions necessary to observe also line emission in SBSL.

In this view the aim of the present work was to study and characterize SBSL spectra in the presence of spectroscopically

active probes (Na) and also try to provide further support to the studies^{10–12} on similarities between single-bubble and multibubble sonoluminescences. Therefore, we developed an acoustic bubble trap where temperature, gas nature, gas concentration, and acoustic pressure can be controlled and coupled it to a high-resolution spectroscopic system. We used this setup to measure SBSL spectra of water, NaCl solutions, and sodium dodecylsulfate (SDS) solutions in the presence of different argon concentrations within the acoustic pressure range of stable SBSL (1.0–1.5 bar). The collected spectra are characterized by fitting the broad-band continuum with Planck's law to determine the radiators blackbody temperature T_{bb} as was done by several groups for SB and MBSL,^{13–16} who obtained temperatures between 6000 and 20 000 K. Besides, the appearance of line emissions is studied, together with its dependence on the acoustic pressure and on the interfacial ion concentration.

Experimental Section

The experimental setup for measuring the SBSL spectra consists of a cylindrical quartz resonator cell coupled to a spectroscopic system and is described in detail in the Supporting Information. Furthermore, the Supporting Information includes a literature overview of the geometries of resonator cells used for SBSL studies and describes the development of our resonator cell. In total four different geometries were tested, and the main parameters for a high acoustic pressure field inside the liquid were identified. The final cell is 52 mm in diameter and 90 mm in height. A piezo ceramic transducer (PZT) is glued on its glass bottom. The voltage at the PZT is controlled via a wideband power amplifier (Krohn-Hite model 7500) and a linear sweep-function generator (Linear Krohn-Hite, model 1200A). Due to the capacitor-like behavior of the PZT an inductor (L) and a resistance (R) are switched between amplifier and transducer to achieve electrical resonance (more details about the circuit

* To whom correspondence should be addressed. Phone: +33 (0)4 66 33 92 50. Fax: +33 (0)4 66 79 76 11. E-mail: rachel.pflieger@cea.fr.

[†] Max Planck Institute of Colloids and Interfaces.

[‡] Marcoule Institute for Separation Chemistry.

design can be found in the Supporting Information). The driving frequency (27 kHz) is chosen so as to build an acoustic standing wave in the liquid. The acoustic pressure P_{ac} is detected with a needle hydrophone (Dapco Industries, model NP-10-1) coupled to an oscilloscope (HAMEG, HM407, SP107) and placed ~ 5 mm above the pressure antinode. The needle hydrophone is calibrated against a PVDF hydrophone (RP-acoustics, PVDF hydrophone type 1). Despite the large uncertainty in the determination of the acoustic pressure (± 0.2 bar), the obtained pressures are internally consistent within each of the data sets. The temperature of the sample is kept constant during measurements (14 °C) thanks to a silicon tube wound around the cylindrical cell and connected to a cryostat. Spectroscopic measurements are performed in the range of 200–700 nm with an Acton Research SP-300i imaging spectrometer coupled to a charge-coupled-device detector (PIXIS 100B, Princeton Instrument). The spectrometer is equipped with two gratings: 600 gr/mm blz. 300 nm and 300 gr/mm blz. 500 nm. For measurements in the visible range a high-pass filter at 320 nm is utilized. The light source is imaged on the entrance slit of the spectrometer by a UV-to-NIR-corrected triplet lens (Edmund optics). The wavelength calibration is performed with a Hg(Ar) pen ray light source (LSP 035, LOT). All spectra are acquired at a slot width of 500 μm with a maximal exposure time of 5 min. Spectra are corrected against spectra of a calibrated standard halogen lamp (LOT model LSK113). In the UV range an uncertainty remains essentially due to the curvature of the quartz cylinder.

For all solutions deionized water (0.055 $\mu\text{S}/\text{cm}$) is used. Sodium chloride (Merck) and sodium dodecylsulfate (SDS, Alfa Aesar) are of analytical grade. The final solutions are filtered with a 0.2 μm filter (Whatman, FP 30/0.2 CA-S). A 106 mL amount of the solution is filled into the resonator cell, giving a liquid height of 5 cm, and degassed to a pressure < 24 mbar for at least 30 min using a mechanical pump while stirring. Then the pressure in the cell is increased from 24 to 100 mbar using argon ($> 99.999\%$) (except for measurements with an argon pressure of ~ 1 mbar) and left for equilibration for 30 min while stirring. This process leads to an Ar concentration of 4 mg/L, calculated with Henry's law. Finally, the argon pressure over the solution is increased to atmospheric pressure to allow introduction of a gas bubble (using a syringe) after tuning the ultrasound frequency to the resonance of the cell.

Results

Figure 1 presents SBSL spectra in water pre-equilibrated with argon at ~ 1 and 70 mbar and different acoustic pressures. In the case of a very low argon pressure the spectrum consists of a broad continuum whose intensity increases with increasing acoustic pressure. The shape of this continuum resembles blackbody emission and can be fitted using Planck's law (eq 1) to determine the corresponding blackbody temperatures

$$I = \varepsilon C_1 \lambda^{-5} / [\exp(C_2/\lambda T) - 1] \quad (1)$$

where ε is the emissivity, C_1 and C_2 are constants (equal to, respectively, 37 418 ($\text{W } \mu\text{m}^4/\text{cm}^2$) and 14 388 $\mu\text{m K}$),¹⁷ the wavelength λ is in μm , and the intensity I is in $\text{W}/(\text{cm}^2 \mu\text{m})$. Assuming that $C_2/\lambda T \gg 1$, eq 1 can be simplified and linearized into eq 2

$$\ln(\lambda^5 I) - \ln(\varepsilon C_1) = -C_2/(\lambda T) \quad (2)$$

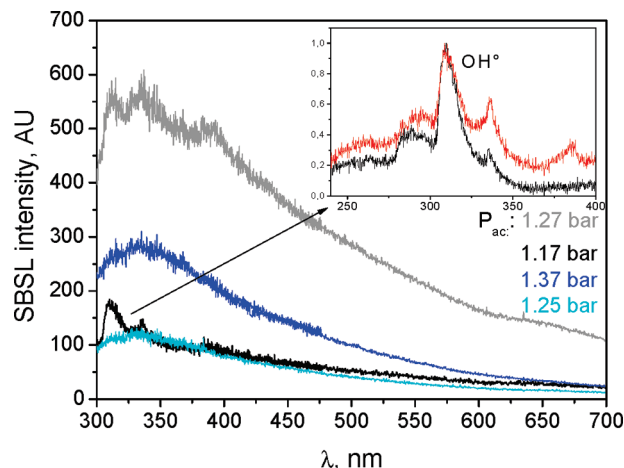


Figure 1. SBSL spectra in water with ~ 1 mbar Ar (blue, light blue) and 70 mbar Ar (gray, black) at various P_{ac} . (Inset) Enlarged OH^* peak in water (black) and in 0.5 M NaCl (red) with 70 mbar of Ar.

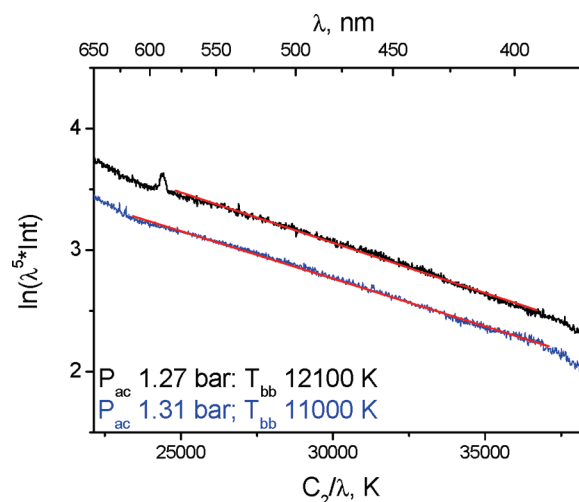


Figure 2. Linearized spectra of SBSL in water (blue) and 0.5 M NaCl (black) with 70 mbar Ar fitted linearly (red).

Assuming that the emissivity is constant, eq 2 describes a straight line in the coordinates $x = C_2/\lambda$ and $y = \ln(\lambda^5 I)$, the slope of which gives the corresponding blackbody temperature (T_{bb}).

Curves obtained in water and in a 0.5 M NaCl solution are exemplified in Figure 2, and derived blackbody temperatures for three different acoustic pressures are given in Table 1. For water pre-equilibrated with ~ 1 mbar of argon at room temperature T_{bb} is ~ 17 100 K. It is not dependent on the applied acoustic pressure. When the argon pressure is increased to 70 mbar, as optimized by Liang,¹⁰ T_{bb} decreases to ~ 11 100 K. When a NaCl solution under 70 mbar of Ar is considered, T_{bb} is similar to the value obtained in pure water. Besides the continuum the SBSL spectra of water with an argon pressure of 70 mbar exhibit a line emission at 310 nm (inset in Figure 1) with a shoulder around 280 nm. It corresponds to the emission of excited OH^* radicals ($\text{A}^2\Sigma^+ - \text{X}^2\Pi$).¹⁸ Two other lines are observed at 336 and 385 nm. The origin of these lines is not clear but is in agreement with the lines observed by Young.⁹ The line at 336 nm disappears when the liquid is degassed for 1 h, indicating the influence of traces of air.

Figure 3 shows SBSL spectra obtained at different acoustic pressures in a 0.5 M NaCl solution regassed with 70 mbar of argon. Similar spectra are obtained with NaCl concentrations of 1, 2, and 3 M. The spectra at low acoustic pressures present

TABLE 1: T_{bb} (in K, fit uncertainty 300 K) vs P_{ac} in Degassed Water and in Water with 70 mbar of Argon (Figure 1) and in 0.5 M NaCl with 70 mbar of Argon (Figure 3)^a

	acoustic pressure (bar), ± 0.2	T_{bb} (K), ± 300 K
0.5 M NaCl 70 mbar Ar	1.27	11 000
	1.20	11 800
	1.19	11 400
water 70 mbar Ar	1.31	11 000
	1.27	10 800
	1.13	11 500
degassed water	1.37	16 700
	1.35	17 600
	1.23	17 100

^a Fitting range approximately 320–600 nm; estimated amount of argon in degassed water ~ 1 mbar.

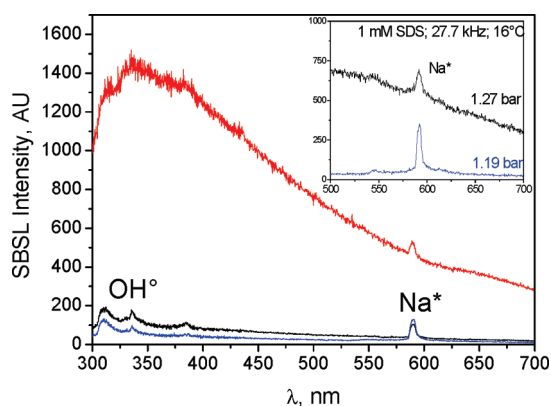


Figure 3. SBSL spectra in 0.5 M NaCl regassed with 70 mbar Ar at P_{ac} of 1.25 (red), 1.20 (black), and 1.13 bar (blue). (Inset) 1 mM SDS with 70 mbar of Ar at P_{ac} of 1.27 and 1.19 bar.

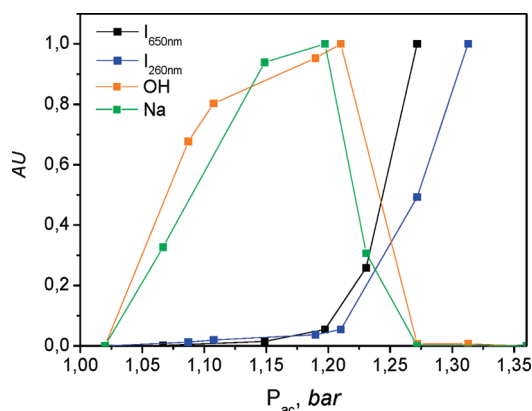


Figure 4. Evolution with P_{ac} of peak heights of OH^* and Na^* and of the continuum represented by SBSL intensities at 650 and 260 nm in 0.5 M NaCl, 70 mbar argon.

two line emissions: one at 310 nm with a shoulder at 280 nm which is identical to the line observed in water with 70 mbar argon (inset Figure 1) and a second line at 589 nm attributed to sodium emission.¹⁹ The sodium line is accompanied by a satellite peak at 545 nm. The line intensities increase with increasing P_{ac} until 1.2 bar as visualized in Figure 4, and then they decrease until becoming indistinguishable from the continuum. Note that all intensities were normalized to their maximum value. In Figure 4 the continuum is represented by the SL intensities at 260 and 650 nm. At a very low concentration of NaCl (1 mM) no Na line emission is observed. By contrast, this line is clearly visible in a solution of SDS with a concentration of 1 mM but

without any additional NaCl (inset in Figure 3). It is to be noted that SDS quenches the OH^* line emission and the broad SBSL continuum as shown in Figure S5, Supporting Information.

Discussion

Several hypotheses have been proposed to describe the origin of SBSL among which is the generation of a hot spot from a quasi-adiabatic heating that can be described by blackbody radiation.²⁰ We used the latter model to determine the blackbody temperatures (T_{bb}) of a single cavitation bubble at different acoustic pressures and different argon pressures in water and in aqueous solutions of sodium chloride. Fits of SBSL spectra in water with ~ 1 mbar of argon pressure yield blackbody temperatures of $\sim 17\,000$ K whatever the acoustic pressure. This value is in a good agreement with T_{bb} determined by Simon et al.,²¹ who studied SBSL under similar experimental conditions. When the argon pressure in solutions is increased to 70 mbar a significantly lower blackbody temperature (11 000 K) is obtained that is also independent of the acoustic pressure. At the same argon pressure and in the presence of NaCl the temperature remains the same.

Thus, the blackbody temperatures appear to be independent of the salt concentration and the applied acoustic pressure, whereas the SL intensity is very sensitive to these parameters as shown here and in several other studies.^{10,22–24} For example, the SL intensity increases by a factor of ~ 10 within the range of stable SBSL. In the case of water with 1 mbar Ar this observation may be explained by changes in the bubble radius at collapse (which changes by approximately a factor of 2 in the studied acoustic pressure range for degassed water²⁵) and by changes in the light pulse duration that also changes by a factor of 2 for degassed water.²⁶ Such arguments may also explain that the SL intensity can be higher with 70 mbar Ar than with 1 mbar Ar, although the derived blackbody temperature is significantly lower. Indeed, both the minimum radius and the pulse width are expected to increase as the noble gas content of the liquid is increased.²⁷ However, it does not explain why almost the same temperature ($12\,500 \pm 1500$ K²⁸) was determined by blackbody fitting of SBSL in concentrated H_2SO_4 , although the SL intensity in concentrated sulfuric acid is 2700 times higher than that in water.¹² This apparent discrepancy questions the application of the blackbody model on sonoluminescence spectra and requires further dedicated studies.

The spectra of sodium chloride solutions at 70 mbar of argon exhibit two striking features. The first one, as outlined by Liang,¹⁰ is that only at argon pressures of some tens of mbar the SL continuum exhibits line emissions of OH^* and Na^* . The acoustic pressure threshold for radical production and sodium reduction and excitation is above the threshold for stable cavitation, which is in the range of 0.8–0.9 bar depending on the experimental conditions, and slightly below the threshold for the emission of the broad-band continuum. We followed the evolution of the peak heights and continuum intensity as shown in Figure 4. In the first domain of acoustic pressure ($P_{ac} < 1.2$ bar) both the line intensities and the continuum are increasing (Figure 4), which is consistent with more extreme conditions within the bubble with increasing acoustic pressure. Above 1.2 bar the continuum increases much faster, concomitant with a drastic decrease of the line emissions. This striking result can be explained by nonradiative deactivation of excited OH^* and Na^* with increasing acoustic pressure arising from a quenching by hot particles issued from a plasma core.¹⁶

The second striking feature is the appearance of two vibrational electronic transitions of OH^* radicals: at 310 nm,

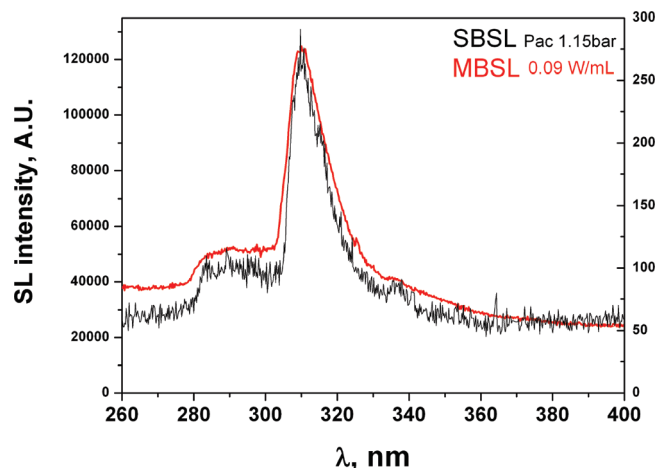


Figure 5. OH^* ($\text{A}^2\Sigma^+ - \text{X}^2\Pi$) emission peak in SBSL 27 kHz and MBSL 20 kHz obtained in water with argon (70 mbar argon for SBSL, argon flow 5.3 L/h for MBSL).

assigned to $\text{A}^2\Sigma^+(\nu=0) \rightarrow \text{X}^2\Pi(\nu=0)$ and at 280 nm assigned to $\text{A}^2\Sigma^+(\nu=1) \rightarrow \text{X}^2\Pi(\nu=0)$ ²⁹ (inset Figure 1). The OH^* emission is identical to that observed in MBSL of water sparged with an argon flow of 5.3 L/h at 20 kHz (Figure 5).³⁰ It is noteworthy that the strong similarity in the shapes of SL spectra of OH^* radicals for SBSL and MBSL indicates similar populations of vibrational exciting states for these species in single-bubble and multibubble systems. In other words, the electronic vibration structure of OH^* lines reveals the similarity in the intrabubble conditions for SBSL and MBSL under conditions favorable for the appearance of line emission in SBSL spectra similar to that observed by Liang.¹⁰

The emission line at 589 nm observed in SBSL of aqueous sodium chloride solutions with 70 mbar argon is attributed to the 3p–3s transition of Na^{22} and is accompanied by a satellite peak at 545 nm (inset Figure 3). The red-shifted satellite peak was already observed in MBSL from water and concentrated sulfuric acid containing Na^+ ,^{31–33} and is assigned to a Na–Ar exciplex. The presence of this exciplex emission implies collisions of sodium and argon atoms and favors according to Lepoint–Mullie³² the concept of collisional excitation of sodium with hot particles in the gas phase of the collapsing bubble.

Line emission in SBSL was attributed by Hatanaka³⁴ to a dancing bubble at high gas concentration. Under similar conditions Krefting observed the formation of daughter bubbles.³⁵ According to Hatanaka et al.,³⁶ tiny bubbles emitted from a larger bubble show sodium line emission in MBSL. However, in our studies the gas concentration is lower, similar to that of Liang et al., who also did not observe any translational movement of the bubble (actually they even saw line emission at much lower argon pressure, down to 7 mbar).¹⁰

Jittering of the bubble is also observed at high salt concentration;³⁷ at low concentrations (like 0.5 M) moving sets in at high acoustic pressures. In the present study, line emission of sodium and hydroxyl is observed at all NaCl concentrations (starting with 0.5 M) and these lines are especially intense at low acoustic pressures. Thus, it appears that either the translation is in the microscopic scale or a nondancing bubble can also produce line emission.

Note here that Na line emission is not observed in SBSL spectra of a 1 mM NaCl solution, whereas it is clearly visible in a 1 mM solution of SDS. As in former studies of MBSL in the presence of a surfactant³⁸ the enhanced emission of sodium is ascribed to the adsorption of surface-active dodecylsulfate at

the cavitation interface enriching it with sodium ions. The spectra emphasize the importance of the ion concentration at the interface of the cavitation bubble (inset of Figure 2). At the same time SL is quenched in the presence of SDS as it is shown in Figure S5 of Supporting Information. Such a quenching was also observed in studies of MBSL, though at a higher SDS concentration, going along with a strong reduction of the hydrogen peroxide production,³⁹ which was traced back to scavenging of OH^* radicals by the pyrolysis products of SDS adsorbed at the interface. Endothermic pyrolysis of SDS also quenches the SL continuum.³⁹ The mechanism and site (either in the gas phase⁴⁰ or in the heated interfacial area⁴¹ of the hot spot) of the OH^* quenching and formation of excited metal atoms cannot be identified yet and require further research.

Conclusions

Aiming to quantify the conditions created in the gas phase and at the interface of a cavitation bubble in water and NaCl solutions we used blackbody fits to characterize the sonoluminescence spectra obtained from a single bubble at 27 kHz. The blackbody temperatures obtained are in the range of 11 000 K for an Ar pressure of 70 mbar and 17 000 K for an Ar pressure of ~ 1 mbar. They are independent from the acoustic pressure, whereas the SL yield increases more than 10-fold with increasing acoustic pressure. These observations can be interpreted by means of an increase in the bubble radius at collapse. In some particular conditions light emission from OH^* radicals and Na^* is observed. The shape of the OH^* peak is identical to that obtained in MBSL at low-frequency ultrasound of 20 kHz and reveals the similarity between conditions created during single-bubble and multibubble sonoluminescence. Furthermore, it is shown using a surface-active counterion that the Na^* line emission in SBSL strongly depends on the interfacial concentration of Na ions. SDS quenches emission from OH^* radicals and the SL continuum. The most striking feature, namely, the drastic decrease of the OH^* and Na^* emission lines intensity at the highest acoustic pressures, is most likely due to enhanced quenching by hot particles formed in a plasma.

Acknowledgment. This work was performed within the framework of LEA SONO between CNRS and MPI-KG. The authors thank Prof. Zemb (ICSM, Marcoule) and Dr. Thomas Kurz (University of Göttingen) for valuable discussions and Henri-Pierre Brau (ICSM, Marcoule) and Dmitry Fix (MPI-KG, Potsdam) for help with the optical system. Special thanks go to Jan von Szada-Borzykowski, Cliff Janiszewski, Dipl. Ing. Henryk Pitas, Dipl. Ing. (FH) Martin Haase, and Bodo Ryschka for help building up the setup.

Supporting Information Available: Literature overview of resonator cells used in SBSL studies, development of resonator cell used in our studies, pictures and properties of the tested resonator cells, an experimental setup diagram, and additional spectra of SBSL in the presence of sodium dodecylsulfate. This material is available free of charge via the Internet at <http://pubs.acs.org>.

References and Notes

- (1) Leighton, T. G. *The Acoustic Bubble*; Academic Press: London, 1994.
- (2) Frenzel, H.; Schultes, H. Z. *Phys. Chem.* **1934**, 27 (5/6), 421.
- (3) Gaitan, D. F.; Crum, L. A.; Church, C. C.; Roy, R. A. *J. Acoust. Soc. Am.* **1992**, 91, 3166.
- (4) Yosioka, K.; Omura, A. *Proc. Annu. Meet. Acoust. Soc. Jpn.* **1962**, 125.

- (5) Flannigan, D. J.; Suslick, K. S. *Phys. Rev. Lett.* **2005**, *95*, 044301/1.
- (6) Eddingsaas, N. C.; Suslick, K. S. *J. Am. Chem. Soc.* **2007**, *129*, 3838.
- (7) Yasui, K.; Tuziuti, T.; Sivakumar, M.; Iida, Y. *Appl. Spectrosc. Rev.* **2004**, *39*, 399.
- (8) Matula, T. J.; Roy, R. A.; Mourad, P. D. *Phys. Rev. Lett.* **1995**, *75*, 2602.
- (9) Young, J. B.; Nelson, J. A.; Kang, W. *Phys. Rev. Lett.* **2001**, *86*, 2673.
- (10) Liang, Y.; Chen, W. Z.; Xu, X. H.; Xu, J. F. *Chin. Sci. Bull.* **2007**, *52*, 3313.
- (11) Didenko, Y. T.; Gordeychuk, T. V. *Phys. Rev. Lett.* **2000**, *84*, 5640.
- (12) Flannigan, D. J.; Suslick, K. S. *Nature* **2005**, *434*, 52.
- (13) Noltingk, B. E.; Neppiras, E. A. *Proc. Phys. Soc. London Sect. B* **1950**, *63*, 674.
- (14) Hiller, R.; Putterman, S. J.; Barber, B. P. *Phys. Rev. Lett.* **1992**, *69*, 1182.
- (15) Vazquez, G.; Camara, C.; Putterman, S.; Weninger, K. *Opt. Lett.* **2001**, *26*, 575.
- (16) Yasui, K. *Phys. Rev. E* **1999**, *60*, 1754.
- (17) Magunov, A. N. *Instrum. Exp. Tech.* **2009**, *52*, 451.
- (18) Mohan, H.; *Shardanand Free radical OH*; National Technical Information Service: Washington, D.C., 1975.
- (19) Bearman, G. H.; Leventhal, J. J. *Phys. Rev. Lett.* **1978**, *41*, 1227.
- (20) Young, F. R. *Sonoluminescence*, 1st ed.; CRC Press: Boca Raton, FL, 2004.
- (21) Simon, G.; Levinsen, M. T. *Phys. Rev. E* **2003**, *68*, 046307/1.
- (22) Winiarczyk, W.; Musiol, K. *Opt. Commun.* **1999**, *172*, 93.
- (23) Tronson, R.; Ashokkumar, M.; Grieser, F. *J. Phys. Chem. B* **2002**, *106*, 11064.
- (24) Barber, B. P.; Hiller, R. A.; Lofstedt, R.; Putterman, S. J.; Weninger, K. R. *Phys. Rep., Rev. Sect. Phys. Lett.* **1997**, *281*, 65.
- (25) Vazquez, G.; Camara, C.; Putterman, S. J.; Weninger, K. *Phys. Rev. Lett.* **2002**, *88*, 197402/1.
- (26) Pecha, R.; Gompf, B.; Nick, G.; Wang, Z. Q.; Eisenmenger, W. *Phys. Rev. Lett.* **1998**, *81*, 717.
- (27) Hopkins, S. D.; Putterman, S. J.; Kappus, B. A.; Suslick, K. S.; Camara, C. G. *Phys. Rev. Lett.* **2005**, *95*, 254301/1.
- (28) Flannigan, D. J.; Suslick, K. S. *Abstr. Pap. Am. Chem. Soc.* **2005**, *229*, 404.
- (29) Sun, B.; Sato, M.; Clements, J. S. *J. Electrostat.* **1997**, *39*, 189.
- (30) Pflieger, R.; Brau, H.-P.; Nikitenko, S. I. *Chemistry* **2010**, *16*, 11801.
- (31) Xu, J. F.; Chen, W. Z.; Xu, X. H.; Liang, Y.; Huang, W.; Gao, X. X. *Phys. Rev. E* **2007**, *76*, 026308/1.
- (32) Lepoint-Mullie, F.; Voglet, N.; Lepoint, T.; Avni, R. *Ultrason. Sonochem.* **2001**, *8*, 151.
- (33) Flannigan, D. J.; Suslick, K. S. *Phys. Rev. Lett.* **2007**, *99*, 134301/1.
- (34) Hatanaka, S.; Mitome, H.; Yasui, K.; Hayashi, S. *J. Am. Chem. Soc.* **2002**, *124*, 10250.
- (35) Krefling, D.; Mettin, R.; Lauterborn, W. *Fortschr. Akustik DAGA* **2001**, 252.
- (36) Hatanaka, S.; Hayashi, S.; Choi, P. K. *Jpn. J. Appl. Phys.* **2010**, *49*, 07HE01/1.
- (37) Nozaki, K.; Hatanaka, S.; Hayashi, S. *Jpn. J. Appl. Phys., Part 1* **2004**, *43*, 6481.
- (38) Grieser, F.; Ashokkumar, M. *Adv. Colloid Interface Sci.* **2001**, *89*, 423.
- (39) Sunartio, D.; Yasui, K.; Tuziuti, T.; Kozuka, T.; Iida, Y.; Ashokkumar, M.; Grieser, F. *ChemPhysChem* **2007**, *8*, 2331.
- (40) Sehgal, C.; Steer, R. P.; Sutherland, R. G.; Verrall, R. E. *J. Chem. Phys.* **1979**, *70*, 2242.
- (41) Flint, E. B.; Suslick, K. S. *J. Phys. Chem.* **1991**, *95*, 1484.

JP1083339